

INVENTORY OF SUPPLEMENTAL INFORMATION

Supplementary Figures:

- Figure S1. Related to Figure 1
- Figure S2. Related to Figure 2
- Figure S3. Related to Figure 3
- Figure S4. Related to Figure 4
- Figure S5. Related to Figure 5
- Figure S6. Related to Figure 6
- Figure S7. Related to Figure 7

Supplementary Tables:

Supplemental Table 1. KLF4 ChIP-seq peaks during reprogramming. Related to Figure 1

Supplemental Table 2. H3K27ac ChIP-seq peaks during reprogramming. Related to Figure 1

Supplemental Table 3. TPM values for RNA-seq in MEF, PSC and different stages of reprogramming. Related to all Figures

Supplemental Table 4. Coordinates of H3K27ac HiChIP MEF-specific loops, PSC-specific loops and constant. Related to Figure 2

Supplemental Table 5. Coordinates of enhancer hubs. Related to Figure 4

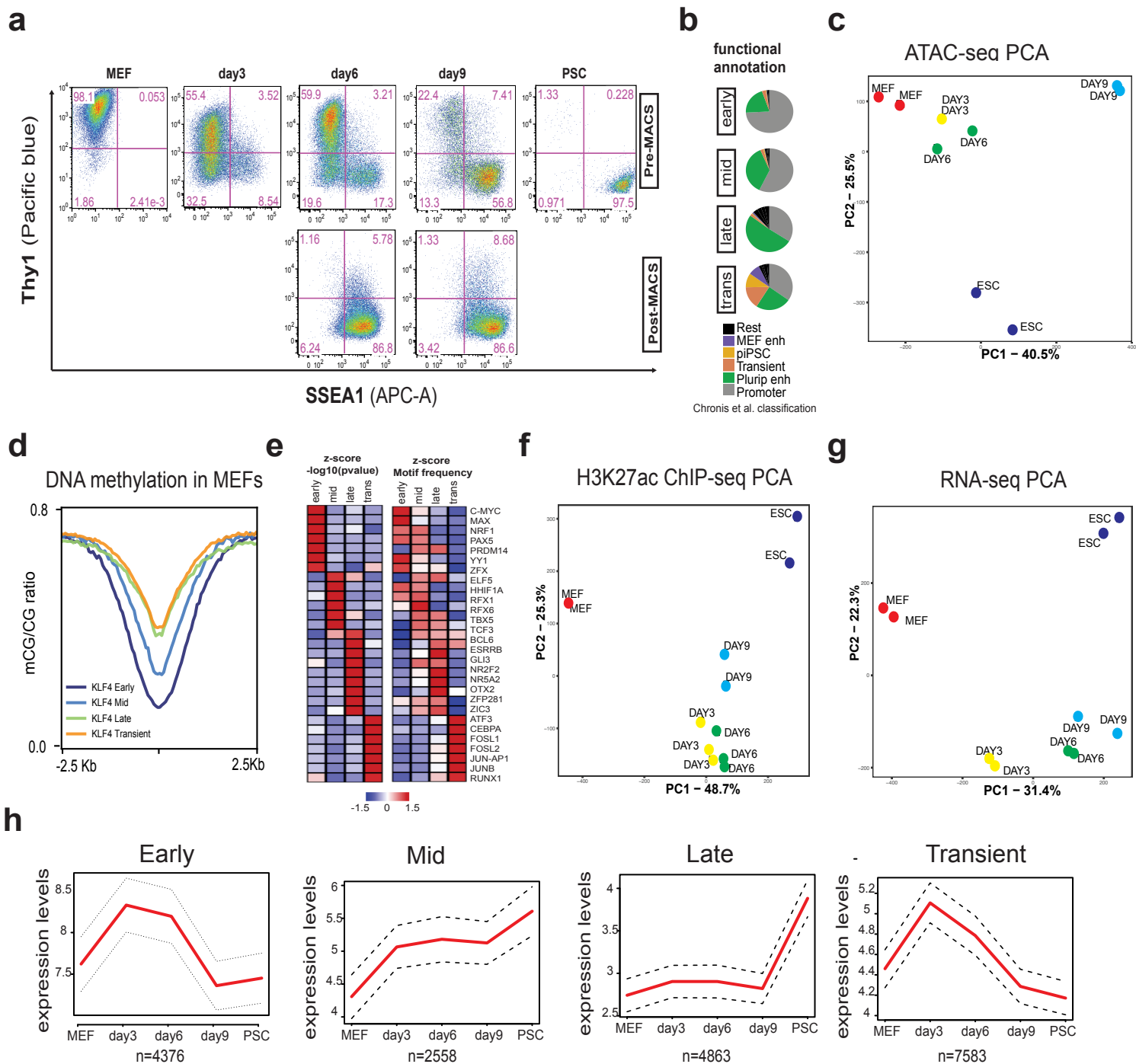
Supplemental Table 6. Coordinates of KLF4 HiChIP gained loops and lost loops, Related to Figure 5

Supplemental Table 7. List of proteins found to interact with KLF4 by RIME. Related to Figure 5

Supplemental Table 8. Coordinates of H3K27ac HiChIP in WT and TKO cells. Related to Figure 6

Supplemental Table 9. Primers and gRNAs used in this study, Related to Figures 4,6 and 7

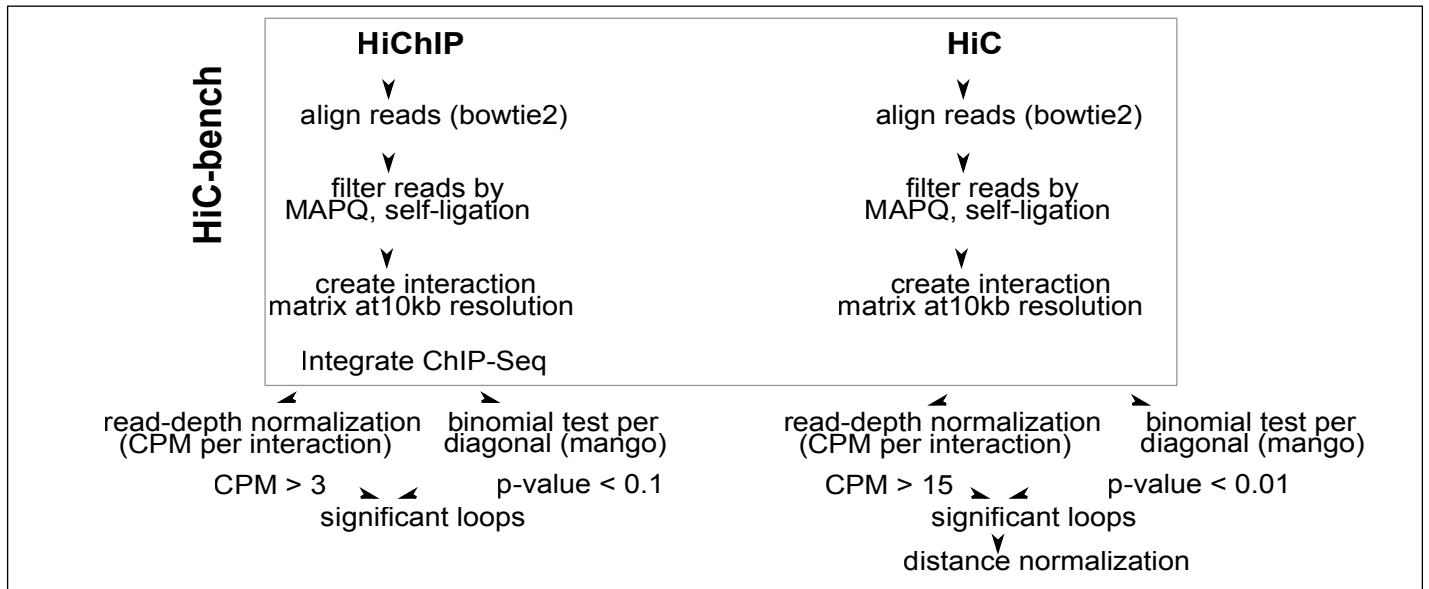
Figure S1



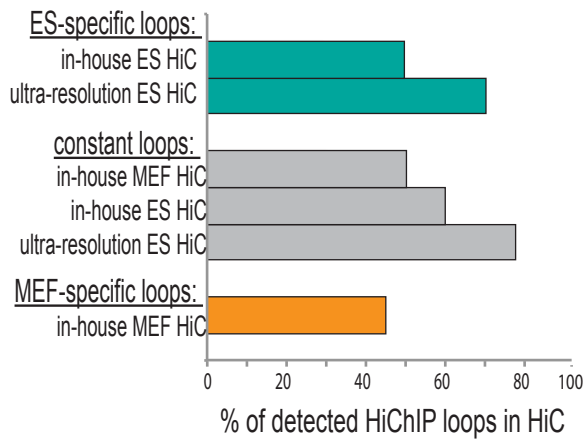
Supplementary Figure 1. **a**, FACS analysis plots showing expression of SSEA1 (early pluripotency marker) and Thy1 (somatic marker) at different stages of reprogramming, before and after SSEA1 enrichment by MACS isolation. **b**, Pie charts of functional classification of KLF4 Early, Mid, Late and Transient peaks (based on Chronis et al. 2017) (piPSC= partial iPSCs). **c**, PCA analysis of ATAC-seq peaks in MEF, PSC and different stages of reprogramming. **d**, Average line plot showing the methylated CG to non-methylated CG ratio from MEF data¹² centered (+/-2.5Kb) around different clusters of KLF4 binding sites (Early, Mid, Late or Transient KLF4 targets, Fig.2b). **e**, Motif enrichment for Early, Mid, Late and Transient KLF4 binding sites. Selected factors are shown and their significance is expressed as Z-score of $-\log_{10}(\text{pvalue})$ (left) or z-score of motif frequency (right). **f**, PCA analysis of H3K27ac ChIP-seq peaks called in MEF, PSC and different stages of reprogramming **g**, PCA of RNA-seq in MEF, PSC and different stages of reprogramming. **h**, Line plots of the median expression (red line) of genes closest to Early, Mid, Late and Transient peaks, expressed as TPM (transcripts per million).

Figure S2

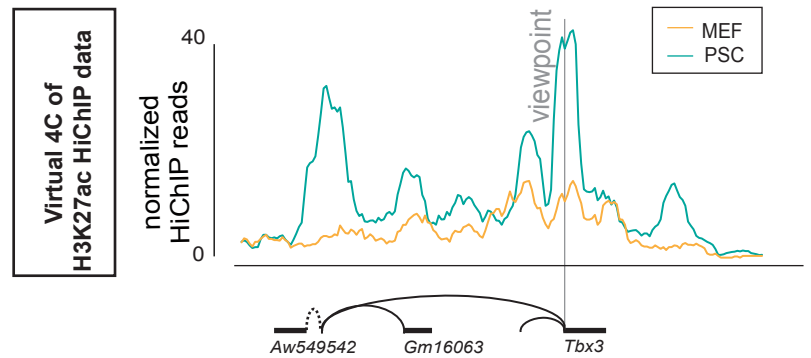
a



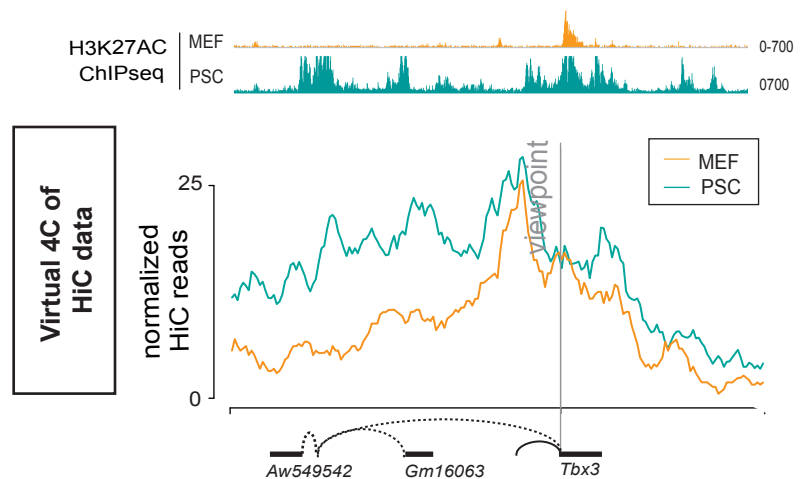
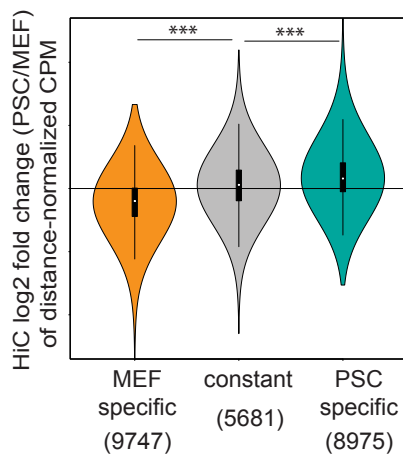
b



c



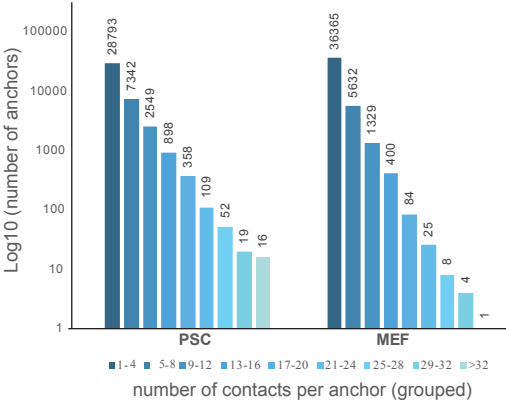
d



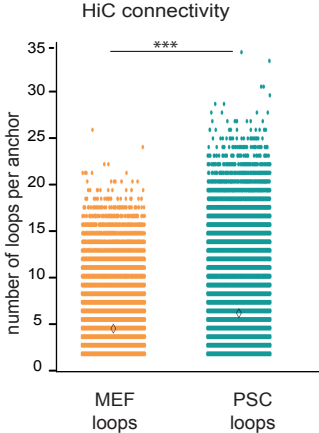
Supplementary Figure 2. a, Schematic work-flow for HiChIP and HiC analysis. **b**, Percentages of PSC-specific, constant or MEF-specific H3K27ac HiChIP loops that were detected in HiC experiments (either generated in-house or published ultra-resolution HiC in PSC³⁸). **c**, Normalized HiChIP (top) and HiC (bottom) signals in MEF and PSC are illustrated in a virtual 4C format around the indicated viewpoint (*Tbx3* promoter). H3K27ac ChIP-seq tracks are shown in MEF and PSC. **d**, Violin plot representing log₂ fold change of distance-normalized HiC signal in PSCs versus MEFs of MEF-specific, constant and PSC-specific loops as called by H3K27ac HiChIP. Only contacts that were detected as significant in HiC data are considered. Numbers of considered loops per category are shown in parenthesis. Unpaired two-sided t-test was used to determine the p-value.

Figure S3

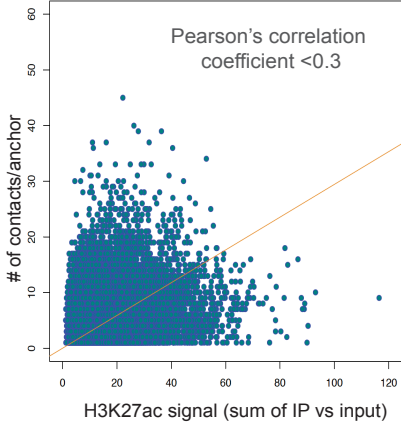
a



b

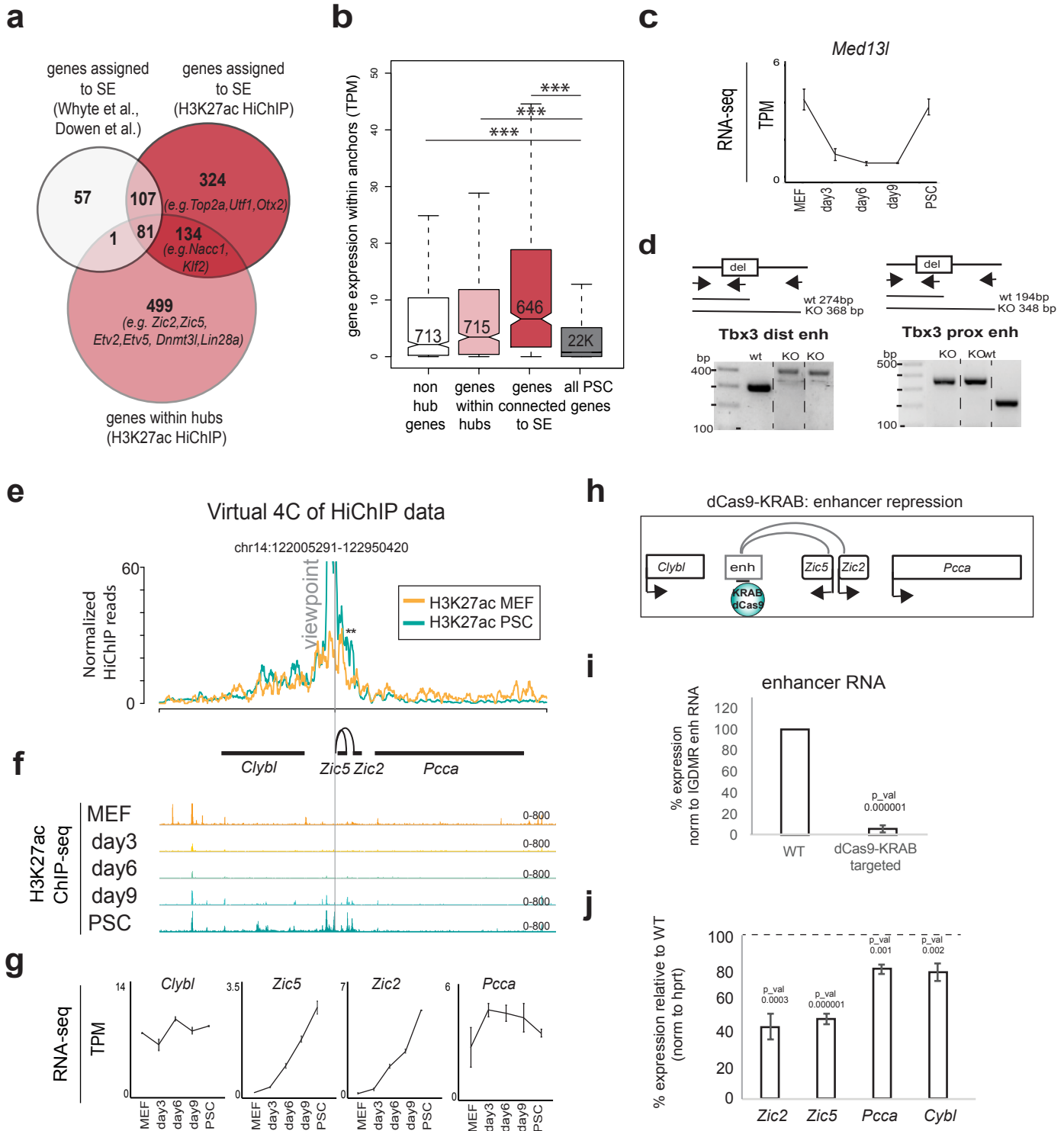


c



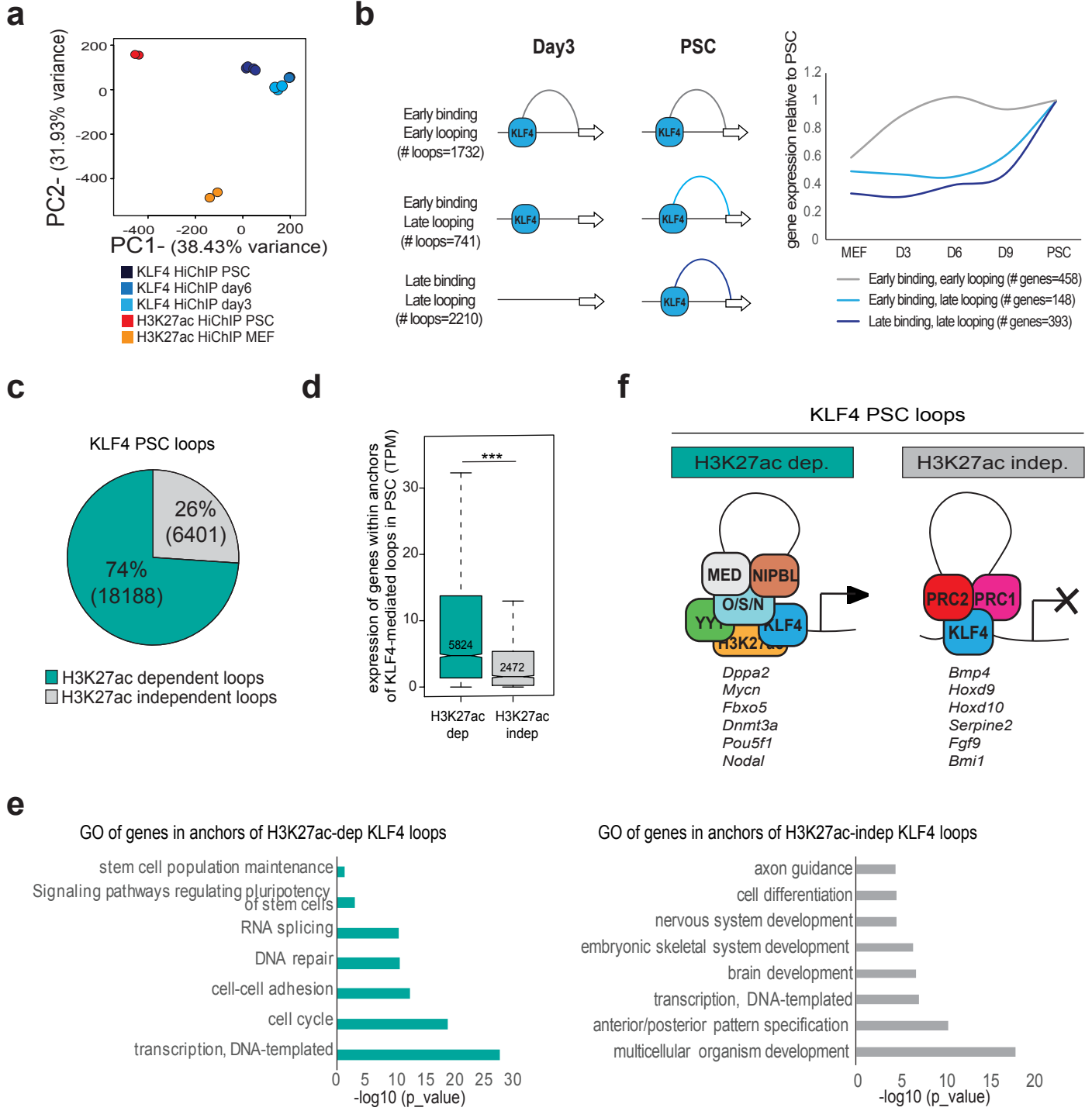
Supplementary Figure 3. **a**, Histogram of anchor connectivity based on H3K27ac MEF and PSC HiChIP called loops. The numbers of contacts per anchor are grouped as shown in the bottom and the actual number of anchors is depicted on top of each bar. **b**, Connectivity of MEF or PSC anchors based on HiC-called loops represented as number of high-confidence contacts around each 10kb anchor. Wilcoxon rank sum test was used to compare connectivity and asterisks indicate significant difference with $p < 0.001$. **c**, Scatter plot showing the correlation of H3K27ac ChIP-seq strength (sum of H3K27ac ChIP/input of all peaks within the anchor) with the number of H3K27ac HiChIP contacts per anchor in PSCs.

Figure S4



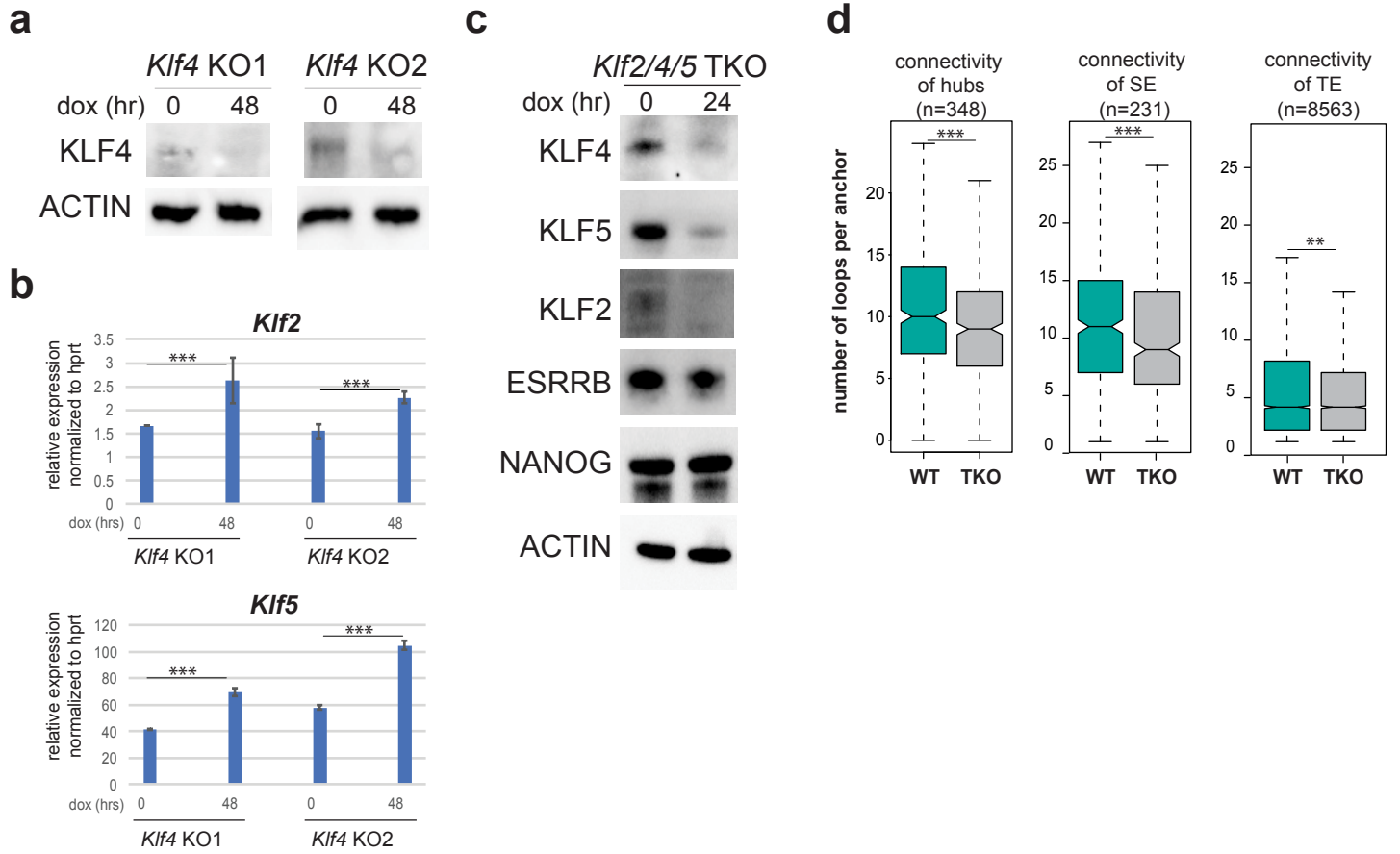
Supplementary Figure 4. **a**, Venn diagram showing overlap between previously assigned target genes for super-enhancers (SE), newly identified SE target genes based on H3K27ac HiChIP contacts in PSCs, and genes connected to PSC-specific enhancer hubs, which represent enhancers contacting more than one gene according H3K27ac HiChIP (see also Fig.4a). **b**, RNA levels of hub genes, non-hub genes or genes connected to SE in PSC samples as measured by RNA-seq and expressed as transcripts per million (TPM). All genes that are not connected to enhancer hubs, but are still detected within PSC-specific HiChIP loops were considered. Expression of all genes expressed in PSC (>1TPM) is shown as reference. **c**, RNA-seq signal (TPM) of *Med13l* -which is not part of the *Tbx3* enhancer hub (see Fig.4b)- during reprogramming **d**, Genotyping strategy and results confirming the homozygous deletion of the distal (left) or the proximal (right) *Tbx3* enhancers. **e**, Example of a newly identified enhancer hub in PSCs. Normalized HiChIP signal around the viewpoint is illustrated as a virtual 4C plot. **f**, H3K27ac ChIP-seq IGV tracks during reprogramming. **g**, RNA-seq signal of genes within the hub (*Zic2* and *Zic5*), or nearby genes (*Clybl* and *Pcca*), are shown for each reprogramming stage to highlight concordance with H3K27ac HiChIP data and coordinated upregulation of genes within the hub. **h**, Schematic illustration of the CRSIPRi (dCas9-KRAB) targeting strategy for inactivation of the *Zic2/Zic5* enhancer hub. **i**, RT-qPCR showing relative levels of the enhancer RNA (normalized to an unaffected enhancer RNA (IGDMR)) in wild type (WT) or dCas9-KRAB-targeted ESCs. P-values were calculated using unpaired one-tailed t-test. Error bars indicate standard deviation from n=2 biological replicates. **j**, RT-qPCR showing expression changes of genes within the hub (*Zic2* and *Zic5*) and nearby genes (*Clybl* and *Pcca*), calculated as percentage relative to WT after normalization to *Hprt* expression. P-values were calculated using unpaired one-tailed t-test. Error bars indicate standard deviation from n=2 biological replicates.

Figure S5



Supplementary Figure 5. **a**, PCA analysis of loops called as significant by H3K27ac and KLF4 HiChIP in different samples. **b**, Left: Chromatin loops that were detected by both KLF4 and H3k27ac HiChIP in PSCs were clustered based on the timing of KLF4 binding and looping during reprogramming. Right: Line plot showing expression changes of genes that belong to each of the indicated loop categories during reprogramming (median values are plotted relative to PSC). **c**, Pie chart showing the percentage of KLF4 PSC loops that were also detected by H3K27ac HiChIP in PSCs (H3K27ac-dependent) or not (H3K27ac-independent). **d**, Boxplot showing expression of genes within all anchors of KLF4-mediated loops that are either H3K27ac-dependent or independent. **e**, Gene ontology for genes within anchors of H3K27ac-dependent or -independent KLF4 loops. **f**, Proposed model for different categories of chromatin loops mediated by KLF4 and cofactors. Example genes are reported for each category.

Figure S6



Supplementary Figure 6. a, Western blot analysis showing KLF4 protein levels before (0) and after (48hr) dox-induction in two ESC clones that harbor dox-inducible CRISPR-Cas9 and gRNAs that target the *Klf4* gene (KLF4 KO1 and KLF4 KO2). **b,** RT-qPCR showing elevated levels of *Klf2* and *Klf5* genes in dox-induced KLF4 KO ESCs. **c,** Western blot showing levels of indicated proteins in a clonal population of ESCs containing an inducible CRISPR-Cas9 construct and gRNAs that target the *Klf2*, *Klf5* and *Klf4* genes. Cells were either untreated (0, wild type or WT cells) or treated with dox for 24 hours (triple knock-out or TKO). **d,** Boxplot showing the connectivity of H3K27ac HiChIP anchors that contain hubs, superenhancers (SE) or typical enhancers (TE) in WT or TKO ESCs. Asterisks indicate significance as calculated using Wilcoxon rank sum test.

Supplementary Figure 7. a, IGV tracks of H3K27ac and KLF4 ChIP-seq in PSCs showing the whole *Tbx3* distal enhancer (top), the region that was deleted by CRISPR/Cas9 (Dist-KO, bottom, see Fig.4f) and the location of the gRNA used to mutate a specific KLF4 binding motif (Dis-KLF4mut gRNA). **b**, Genotyping strategy of the surveyor assay used to detect mutation/indel at the target KLF4 binding site within the distal *Tbx3* enhancer (Dis-KLF4mut). The results for 4 homozygously mutated clones (mut1-4) are shown. **c**, Sequencing results of the four Mut clones compared to the wild type (WT). **d**, ChIP-qPCR showing the relative levels of KLF4 binding to *Tbx3* distal enhancer in two WT clones and four Mut clones (left panel). Values show percentage of ChIP signal over input. As control, binding of KLF4 to an unaffected region (*Fbxo15* promoter) was tested (right panel).